A Highly Efficient and Linear Class-AB/F Power Amplifier for Multimode Operation

Daehyun Kang, Daekyu Yu, Kyoungjoon Min, Kichon Han, Jinsung Choi, *Student Member, IEEE*, Dongsu Kim, Boshi Jin, Myoungsu Jun, and Bumman Kim, *Fellow, IEEE*

***Abstract*—The class-AB/F power amplifier (PA), a multimode PA, which can operate at both class-AB and class-F modes, is analyzed and compared with the conventional class-F and class-AB PAs. The open-circuited third harmonic control circuit enhances the efficiency of the PA without deteriorating the linearity of class-AB mode of the PA. The voltage and current waveforms are simulated to evaluate the appropriate operation for the modes. To demonstrate the multimode PA, the PA is implemented using an InGaP/GaAs HBT process and it is tested with reverse-link IS-95A code division multiple access (CDMA) and PCS1900 global system for mobile communications signals in the personal communications service band. The class-AB operation for a CDMA signal delivers a power-added efficiency (PAE) of 38.9% and an adjacent channel power ratio of −49.5 and −56.5 dBc at the offset of 1.25 and 2.25 MHz, respectively, at the output power of 28 dBm. The maximum PAE of 64.7% under the class-F operation is measured at 32.5-dBm output power for a GSM signal. The class-AB/F PA is a good candidate for the multimode PA of next-generation wireless communication systems.**

***Index Terms*—Class AB, class AB/F, class F, code division multiple access (CDMA), efficient, global system for mobile communications (GSM), handset, heterojunction bipolar transistors (HBTs), IS-95A, linear, monolithic microwave integrated circuit (MMIC), multimode, PCS1900, power amplifier (PA).**

I. Introduction

WIRELESS communication standards have been evolving to meet the market demands for high data rate, mobility, functionality, and low cost. Since different countries have adopted diverse standards, there is a variety of third-generation (3G) wireless communication systems. Moreover, the future generation technology requires that one terminal be used for the multistandards [1]. System technologies for software-defined radio (SDR) have been developed, and RF transceivers have been researched to satisfy the requirements [2], [3]. One of the difficulties in designing such systems is the PA's inability to cover the multimodes of operation.

Wireless communication systems employ either envelope-varying signals or constant-envelope signals. The systems using envelope-varying signals are code division multiple access (CDMA), wideband code division multiple access (WCDMA), EDGE, wireless local area network (WLAN), and WiMAX. These systems modulate the amplitudes of signals to encode more information in the limited bandwidth. Power amplifiers (PAs) working for these systems amplify the input signals linearly, and thus they are called linear PAs [4]. In contrast, the AMPS, global system for mobile communications (GSM), and general packet radio service (GPRS) systems apply constant-envelope signals. Information under these environments is encoded in the phases of signals without changing the amplitudes. Since the PAs for the constant-envelope signals are not required to operate linearly, they are required only to amplify signals efficiently to increase the battery life. In the constant-envelope systems, PAs operate with the output power saturated, and thus they are called saturated PAs.

Therefore, we need a PA operating as a linear PA for an envelope-varying signal and at the same time as a saturated PA for a constant-envelope signal. However, troublesome design issues exist. While the circuit is desired to operate linearly at the backed-off region from the saturated power (P_{SAT}), it should be designed to simultaneously have high efficiency around the P_{SAT}. Efforts have been made to design multimode PAs for the CDMA and AMPS systems [5], [6]. With the classical design of the multimode PAs, however, PAs suffer from direct tradeoffs between linearity and efficiency. The designs focused on the linearity have a deteriorated efficiency for both the linear and saturated PAs. Likewise, improvement on the efficiency degrades the linearity of the linear PAs.

In this paper, we propose a new concept of the multimode class-AB/F PA that operates linearly and efficiently not only for the envelope-varying systems, and efficiently also for the constant-envelope systems. The circuit topology of the PA is based on that of the class-F PA, and the mode of operation is selected by controlling the base bias. The basic operation is explained in Section II. Its operation is further examined by simulation and the design of the PA is explained in Section III. Section IV explains the on-chip implementation through the HBT process to demonstrate the multimode operation for both an IS-95A CDMA and a PCS1900 GSM signals across the personal communications service (PCS) band. The measured results show that the proposed concept is not only realizable, but also leads to high performances under the multimode operation.

Manuscript received August 2, 2007; revised October 14, 2007. This work was supported by the Ministry of Education of Korea under Brain Korea 21 Projects, by the Electronics and Telecommunication Research Institute System-on-Chip Industry Promotion Center, under the Human Resource Development Project for Information Technology System-on-Chip Architect, and by the Ministry of Information and Communication, Korea, under the Information Technology Research Center Support Program supervised by the Institute of Information Technology Advancement (IITA-2007-C1090-0701-0037).

D. Kang, K. Han, J. Choi, D. Kim, B. Jin, M. Jun, and B. Kim are with the Department of Electrical Engineering, Pohang University of Science and Technology (POSTECH), Pohang, Gyungbuk 790-784, Korea (e-mail: daehkang@postech.ac.kr; kichonhan@gmail.com; jinsungc@ieee.org; rookieds@postech.ac.kr; bsjin@postech.ac.kr; msjun@postech.ac.kr; bmkim@postech.ac.kr).

D. Yu and K. Min are with Wireless Power Amplifier Module (WiPAM) Inc., Seongnam, Gyeongi 463-824, Korea (e-mail: dkyu@wipam.co.kr; kjmin@wipam.co.kr).

Color versions of one or more of the figures in this paper are available online at http://ieeexplore.ieee.org.

Digital Object Identifier 10.1109/TMTT.2007.911967

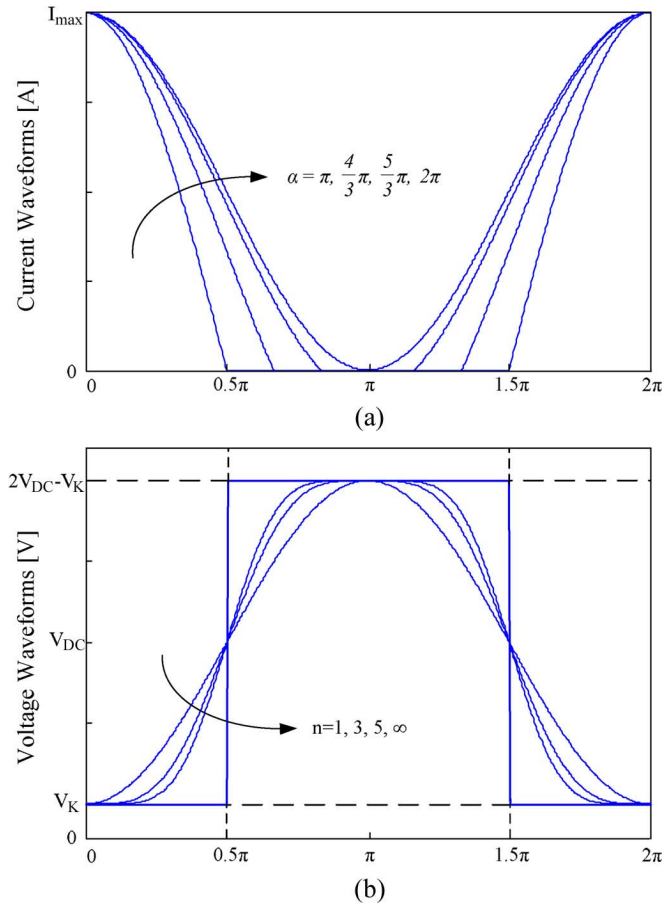

Fig. 1. Current and voltage waveforms of general PAs. (a) Current waveforms as a function of conduction angle (α). (b) Voltage waveforms corresponding to the highest odd harmonic present (n).

II. Concept of Class-AB/F PA

A. General PAs

Operation of general PAs is explained with the waveforms of current and voltage at the current source of the transistor model [7]. Fig. 1(a) shows the current waveforms as a function of conduction angle α. The dc and fundamental components of the current are given by

$$I_{\mathrm{DC}}(\alpha) = \frac{I_{\max}}{2\pi} \cdot \frac{2\sin(\alpha/2) - \alpha\cos(\alpha/2)}{1-\cos(\alpha/2)} \tag{1}$$

$$I_1(\alpha) = \frac{I_{\max}}{2\pi} \cdot \frac{\alpha - \sin\alpha}{1-\cos(\alpha/2)}. \tag{2}$$

The voltage waveforms can be shaped to the square by harmonics, especially by the odd harmonics [8], [9]. Fig. 1(b) illustrates the voltage waveforms affected by the odd harmonics. The value of n indicates the highest odd harmonic present. When the voltage harmonic components have enough power to fulfill the proper ratio, the ratio of the maximum achievable fundamental component to the maximum amplitude for the voltage waveform is defined to be $\delta_V(n)$ as a function of n [10]. The values of $\delta_V(n)$ are

$$\begin{aligned} \delta_V(1) &= 1 \\ \delta_V(3) &= 1.155 \\ \delta_V(5) &= 1.207 \\ \delta_V(\infty) &= \frac{4}{\pi}. \end{aligned} \tag{3}$$

Due to the odd harmonics, the fundamental component of the voltage waveform increases as n increases. The amplitude of the voltage waveform is limited by the knee voltage from the dc level. The maximum amplitude of voltage waveform is $V_{\mathrm{DC}} - V_k$. V_k is the knee voltage of the transistors. Thus, the amplitude of the fundamental voltage is

$$V_1(n) = \delta_V(n) \cdot V_{1\_\max} = \delta_V(n) \cdot (V_{\mathrm{DC}} - V_k). \tag{4}$$

For the maximum power from the PA, the fundamental load impedance is determined to be

$$\begin{aligned} R_1(n,\alpha) &= \frac{\delta_V(n) \cdot V_{1\_\max}}{I_1(\alpha)} \\ &= \frac{\delta_V(n) \cdot V_{1\_\max}}{I_{\max}} \cdot \frac{2\pi \cdot (1-\cos(\alpha/2))}{(\alpha - \sin\alpha)}. \end{aligned} \tag{5}$$

Output power is shown as functions of α and n as follows:

$$P(n,\alpha) = \frac{1}{2} \cdot I_1(\alpha) \cdot \delta_V(n) \cdot V_{1\_\max}. \tag{6}$$

DC power required to obtain the output power is given by

$$P_{\mathrm{DC}}(\alpha) = I_{\mathrm{DC}}(\alpha) \cdot V_{\mathrm{DC}}. \tag{7}$$

Thus, the efficiency is

$$\eta(n,\alpha) = \frac{P(n,\alpha)}{P_{\mathrm{DC}}(\alpha)}. \tag{8}$$

As α increases without any odd harmonic ($n = 1$), class B, AB, and A PAs are determined sequentially. The class-B and class-A PAs have α of π and 2π, respectively; the class-AB PA has an intermediate conduction angle from π to 2π. The ideal class-F PA has a conduction angle of π and all the odd harmonics ($n = \infty$). This leads to efficiency of 100%. In the real case, limited odd harmonics ($n = 3$ or 5) exist because of the difficulty in controlling the high-order terms. Moreover, a bias above the pinchoff is chosen to achieve the proper phase and magnitude relationship between the fundamental and third harmonic voltage components [10].

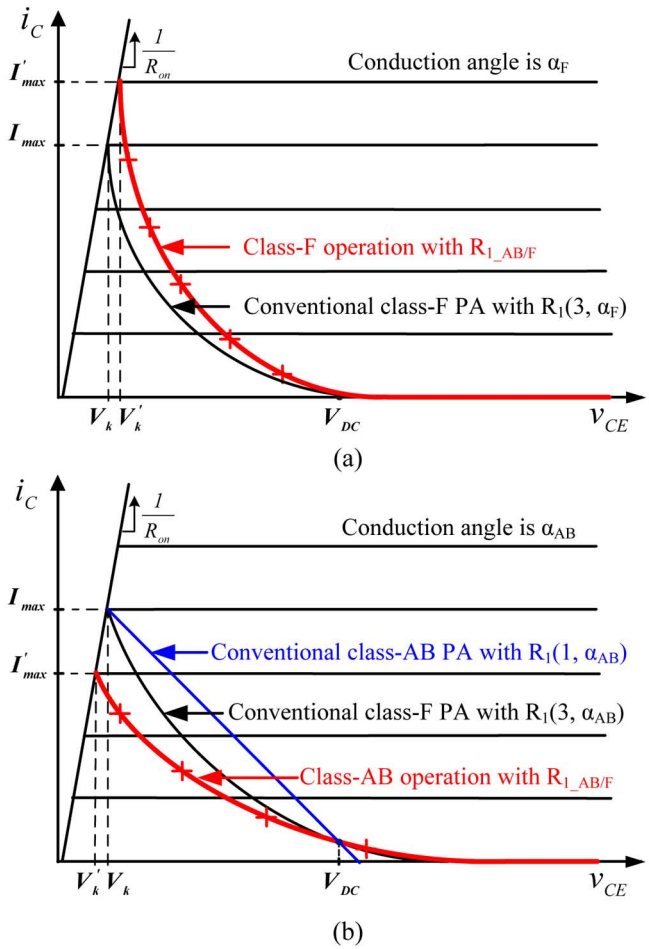

Fig. 2. Load lines for the class-AB/F PA ($n_o = 3$). (a) Class-F operation with the fundamental load $R_{1\_AB/F}$ smaller than $R_1(3, \alpha_F)$ of the conventional class-F PA. (b) Class-AB operation with the fundamental load $R_{1\_AB/F}$ greater than $R_1(1, \alpha_{AB})$ and $R_1(3, \alpha_{AB}$ of the conventional class-AB and class-F PAs.

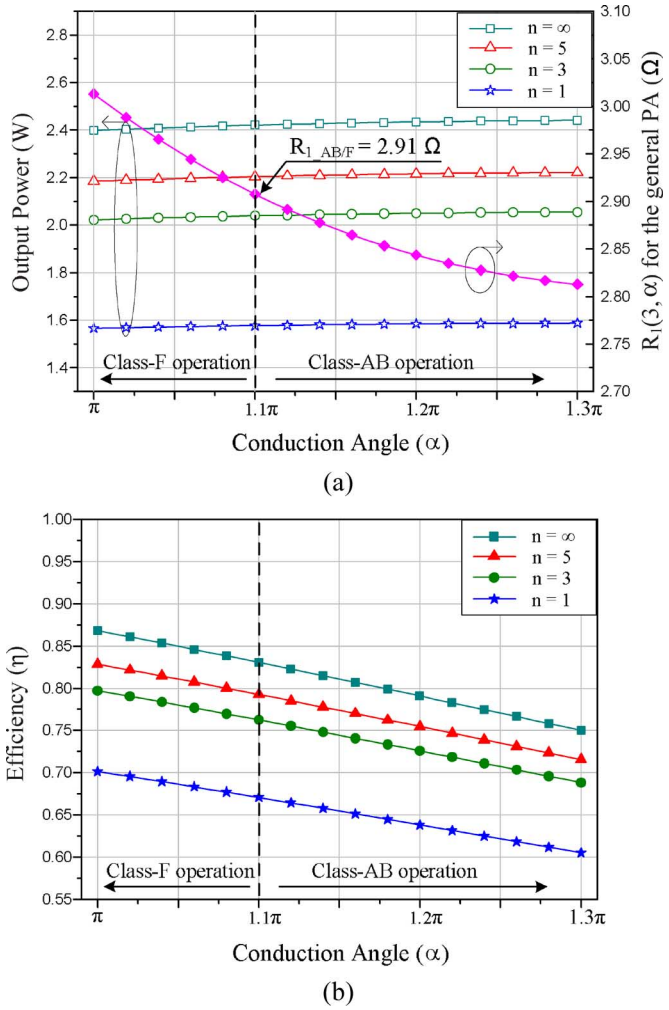

Fig. 3. Performances of the class-AB/F PA as a function of the conduction angle and the odd harmonics, when 2.91 Ω is chosen for $R_{1\_AB/F}$. The PA is in class-F and class-AB operations, respectively, when the α's are close to π and greater than 1.1π. $I_{max} = 2.3$ A, $V_{DC} = 3.4$ V, and $V_k = 0.4$ V. (a) Output power and general PA's fundamental load $R_1(3, \alpha)$. (b) Efficiency.

B. Class-AB/F PA

The class-AB/F PA is a multimode PA with an intermediate fundamental load to achieve both the class-AB and class-F operations. The load impedance of the PA is fixed and the value of the fundamental load $R_{1\_AB/F}$ is located at

$$R_1(n_o, \alpha_F) > R_{1\_AB/F} > R_1(n_o, \alpha_{AB}). \tag{9}$$

where α_F and α_{AB} are the conduction angles for the class-AB and class-F operations, respectively, and n_o is the highest odd harmonic present. $R_1(n_o, \alpha_F)$ and $R_1(n_o, \alpha_{AB})$ are the fundamental loads of the class-F PA with conduction angles of α_F and α_{AB}, respectively [11]. α_F is above, but near, π, and α_{AB} is at a class-AB bias level. The harmonics are tuned up to n_oth order. Fig. 2 shows the load lines of the class-AB/F PA. With the fundamental load of $R_{1\_AB/F}$, the fundamental voltage and current of the class-AB/F PA are determined. The amplitude of the fundamental voltage is

$$V'_1(n_o) = \delta_V(n_o) \cdot (V_{DC} - V'_k) = R_{1\_AB/F} \cdot I'_1(\alpha). \tag{10}$$

As the maximum amplitude of the current is changed, the knee voltage is given by

$$V'_k = R_{on} \cdot I'_{max} = R_{on} \cdot 2\pi \cdot \frac{1 - \cos(\alpha/2)}{\alpha - \sin\alpha} \cdot I'_1(\alpha) \tag{11}$$

where R_{on} is the on resistance. By substituting (10) for V'_k in (11), the fundamental component of the current waveform is given by

$$I'_1(\alpha) = \frac{\delta_V(n_o) \cdot V_{DC}}{R_{1\_AB/F} + \delta_V(n_o) \cdot R_{on} \cdot \frac{2\pi\,(1 - \cos(\alpha/2))}{\alpha - \sin\alpha}}. \tag{12}$$

This gives I'_{max} from (2). The dc current of class-AB/F PA is I'_{DC} from (1), which gives the dc power $P'_{DC}(\alpha)$. The output power and the efficiency of the class-AB/F PA are given by

$$P_{AB/F}(n_o, \alpha) = \frac{1}{2} \cdot I'_1(\alpha) \cdot V'_1(n_o)$$
$$\eta_{AB/F}(n_o, \alpha) = \frac{P_{AB/F}(n_o, \alpha)}{P'_{DC}(\alpha)}. \tag{13}$$

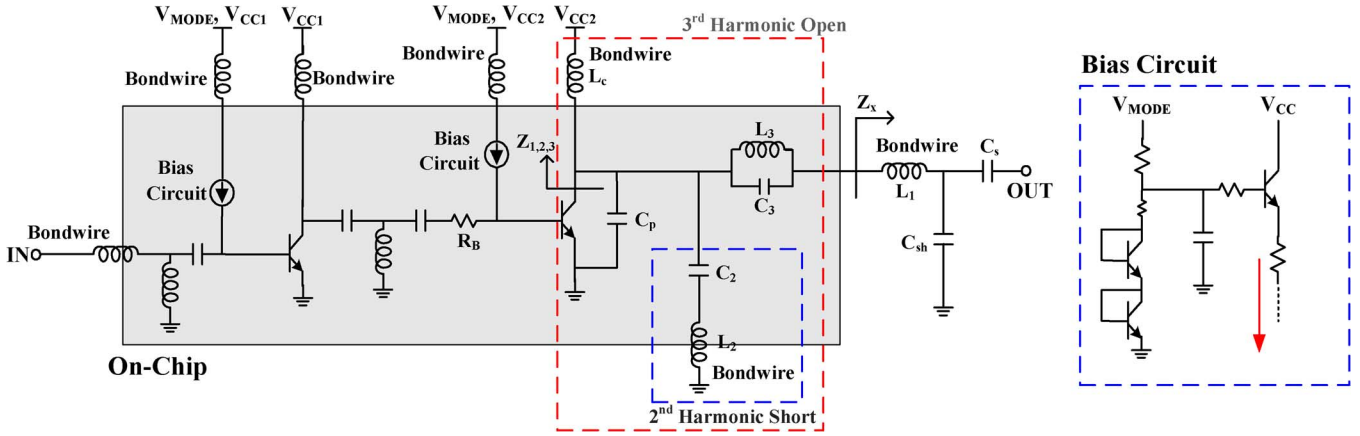

Fig. 4. Schematic of the class-AB/F PA.

The PA operates in the class-AB and the class-F modes when the α's are $\alpha_{\rm AB}$ and $\alpha_{\rm F}$, respectively. The fundamental voltage $V_1'(n_o)$ of the class-F operation is less than $V_1(n_o)$ of the conventional class-F PA, as shown in Fig. 2(a) because of the lower load resistance $R_{1\_{\rm AB/F}}$, and the class-F operation of the PA has lower gain and efficiency than the class-F PA. In contrast, $V_1'(n_o)$ of the class-AB operation is greater than $V-1(1)$ and$V_1(n_o)$ of the conventional class-AB and class-F PAs. The class-AB operation has higher gain and efficiency, but it is less linear than the conventional class-AB PA. The performances of the class-AB/F PA are calculated from (12), and are plotted in Fig. 3. For the same fundamental load of $R_{1\_{\rm AB/F}}$, the class-F operation has higher efficiency and less output power than the class-AB operation. The class-F operation of the PA is nonlinear since it is achieved above, but near, the pinchoff bias level. However, the class-AB operation of the PA is achieved at a class-AB bias. Thus, the class-AB operation is more linear than the class-F operation. Basically, the linearity of class-AB operation follows that of the conventional class-AB PA. One difference between the topologies of the conventional class-AB PA and the class-AB operation of the PA is the open-circuited third harmonic control circuit, while both PAs have the short-circuited second harmonic control circuit. The third harmonic power is produced by the C_{bc} nonlinearities, g_m and clipping effect of the *I–V* curve [12], [13] and is trapped by the third harmonic control circuit forming a standing wave. The second harmonic power is suppressed. The third harmonic power supports the square voltage waveform without consuming any power, while the current waveform remains as it is. However, there is a feedback path through the capacitance between the base and collector of a transistor, and the third harmonic power feeds back to the base through the capacitance. The third harmonic interacts with the fundamental and second harmonics, regenerating the fourth and fifth harmonics. This deteriorates the characteristic of the fifth-order intermodulation distortion (IMD5), but the effect is insignificant. In contrast, it does not affect the characteristic of third-order intermodulation distortion (IMD3) since IMD3 is not generated due to the second harmonic short circuit. The other advantage of class-AB operation of the PA is that it has lower output harmonics power because the harmonics are trapped by the harmonics control circuits without passing to the output load.

III. Design and Simulation of Class-AB/F PA

A. Topology of the Class-AB/F PA

The class-AB/F PA is designed based on the class-F topology with the harmonic control circuits, as shown in Fig. 4. At the dependent current source of transistor, the second harmonic impedance is zero using a series resonant circuit, and the third harmonic impedance is infinite using a parallel resonant circuit [14], [15] in order to achieve a proper ratio of voltage harmonics [10] as follows:

$$Z_3 = \infty \tag{14}$$

$$Z_2 = 0. \tag{15}$$

At the output stage of the PA, the inductors should be chosen carefully since they cause the loss of output power and occupy a large area on the chip. Thus, small inductances are implemented, or bond wires can replace the lossy inductors. With the chosen inductances, the capacitances for the harmonic control circuits are given by the resonance conditions

$$C_3 = \frac{1}{(3w_0)^2 \cdot L_3} \tag{16}$$

$$C_2 = \frac{1}{(2w_0)^2 \cdot L_2} \tag{17}$$

where w_0 is the operating angular frequency. When the components of L_c, C_p, C_2, and L_2 form an infinite impedance by resonance at the third harmonic frequency, the parallel of C_3 and L_3 becomes an open circuit. C_p is the collector–emitter junction capacitance of the transistor, and the value of L_c is calculated by (14) as follows:

$$X_{c,3w_0} \,\|X_{p,3w_0}\|\, X_{2,3w_0} = \infty \tag{18}$$

where

$$\begin{aligned} X_{c,3w_0} &= j3w_0L_c \\ X_{p,3w_0} &= \frac{1}{j3w_0C_p} \\ X_{2,3w_0} &= j\left(3w_oL_2 - \frac{1}{3w_0C_2}\right). \end{aligned} \tag{19}$$

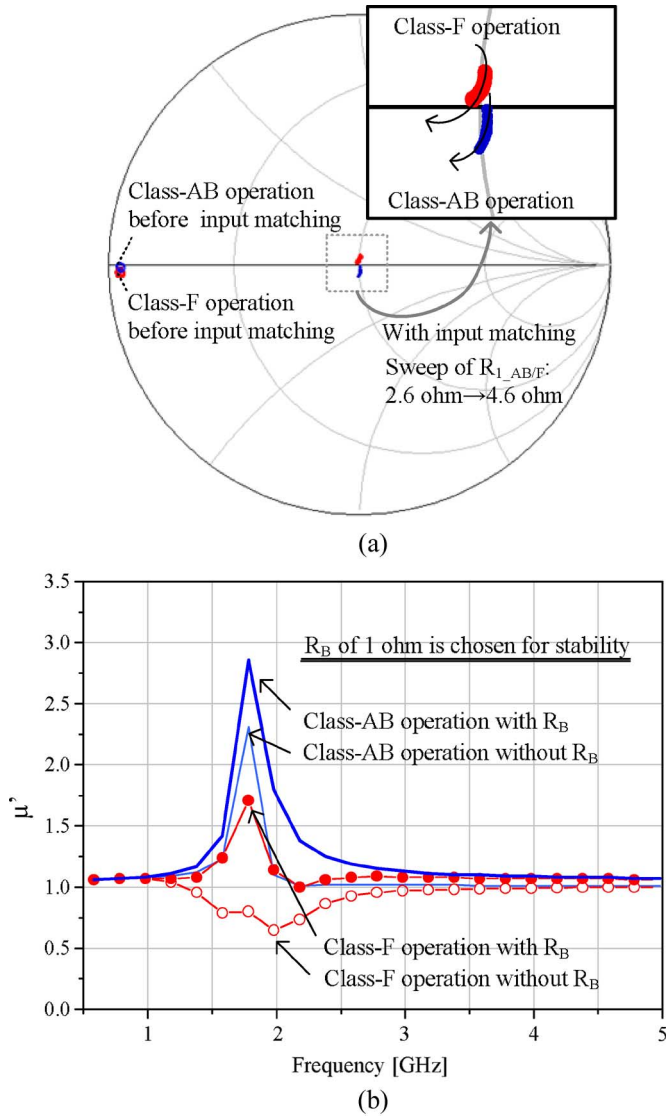

Fig. 5. (a) Input impedance of the power stage with a sweep of $R_{1\_AB/F}$ from 2.6 to 4.6 Ω. (b) μ' parameter for the large-signal stability with/without the ballasting resistor R_B when the input impedance of the power stage is matched. Class-F operation is unstable without R_B.

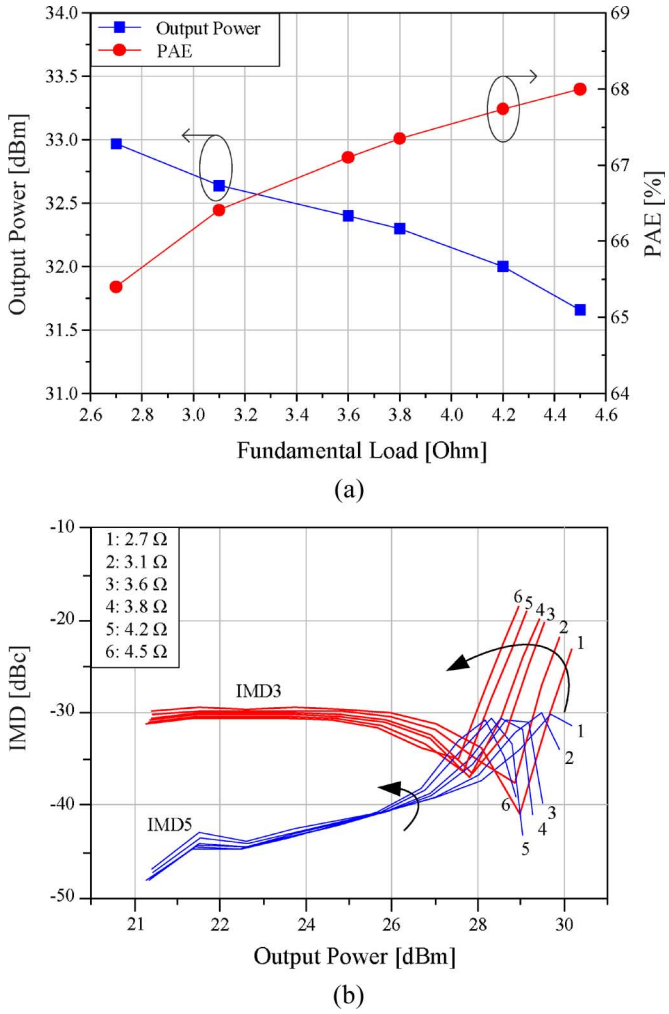

Fig. 6. Determination of the fundamental load $R_{1\_AB/F}$: (a) One-tone test under the class-F operation. (b) Two-tone test under the class-AB operation. The fundamental load of 4.2 Ω is chosen considering the tradeoff between efficiency and linearity.

The series of L_2 and C_2 is inductive at the third harmonic frequency, and the required bond-wire inductance L_c is given by

$$L_c = \frac{L_2'}{(3w_0)^2 \cdot L_2' C_p - 1} \tag{20}$$

where

$$L_2' = L_2 - \frac{1}{(3w_0)^2 \cdot C_2}.$$

The fundamental load impedance $Z_{1\_AB/F}$ at the dependent current source of the transistor is normally a real value given by (9). Assuming that Z_x is matched conjugately to the impedance of components in front of Z_x, the value of Z_x is determined as follows:

$$Z_x = conj\left(R_{1\_AB/F} \| X_c \| X_p \| X_2 + X_3\right) \tag{21}$$

where X_2 and X_3 are the reactance of the third and second harmonic control circuits at the operating frequency. X_c and X_p are the reactance of L_c and C_p, respectively. After Z_x is determined, the output matching components are easily calculated by the normal impedance matching methods.

TABLE I
VALUES OF THE COMPONENTS FOR THE CLASS-AB/F PA

Component	Value [pF]	Component	Value [nH]
C_2	1.79	L_2	1
C_3	7.96	L_3	0.1
C_{sh}	4.5	L_c	1.5
C_s	3.9	L_1	1.15

The class-AB/F PA consists of a drive stage and a power stage, as illustrated in Fig. 4, and the base currents are provided by the active bias circuits [16]. The operation mode of the class-AB/F PA is controlled by the voltage of $V_{\rm MODE}$. A resistor is connected to the emitter of the bias transistor to prevent thermal runaway. Fig. 5(a) shows the input impedance variation of the power stage according to the operation mode and $R_{1\_AB/F}$. The class-AB and class-F operations have different input impedances because of different bias. The inputs of both operations are matched to 50 Ω of resistance. Fig. 5(b) shows the

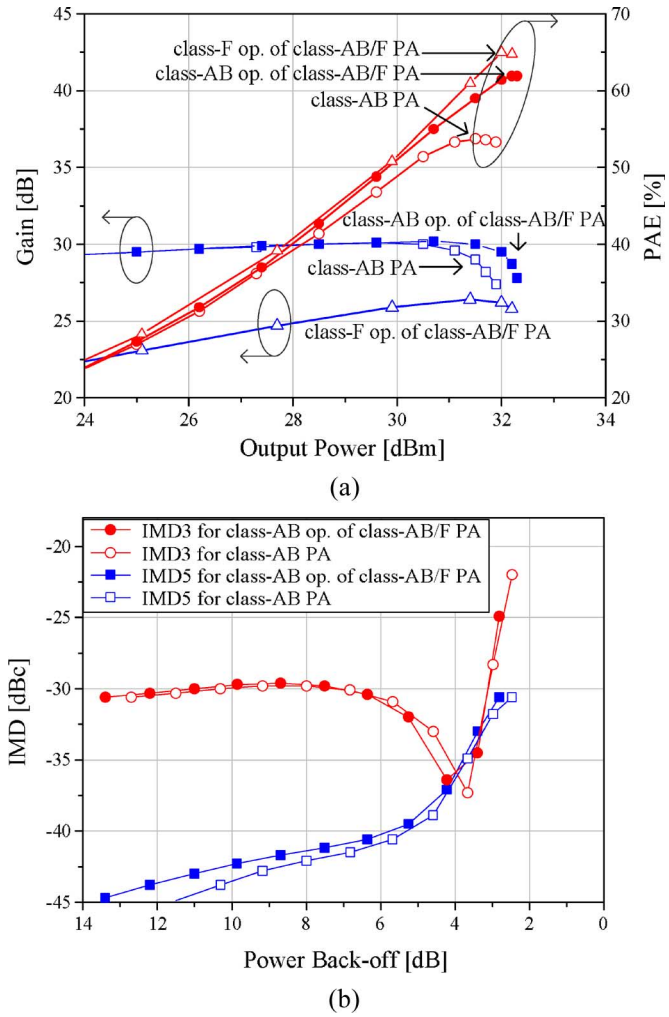

Fig. 7. Simulation results for performance comparison between the class-AB/F PA and the conventional class-AB PA. Supply voltages of 3.4 V and idle currents of 55 and 0.8 mA for the class-AB and class-F operations. (a) One-tone test for the gain and the PAE. (b) Two-tone test with a 2-MHz tone spacing for the IMD characteristics. The power is backoff from the $P1$ dB of 31.6 and 32.1 dBm, respectively, for the conventional class-AB PA and the class-AB operation of the PA.

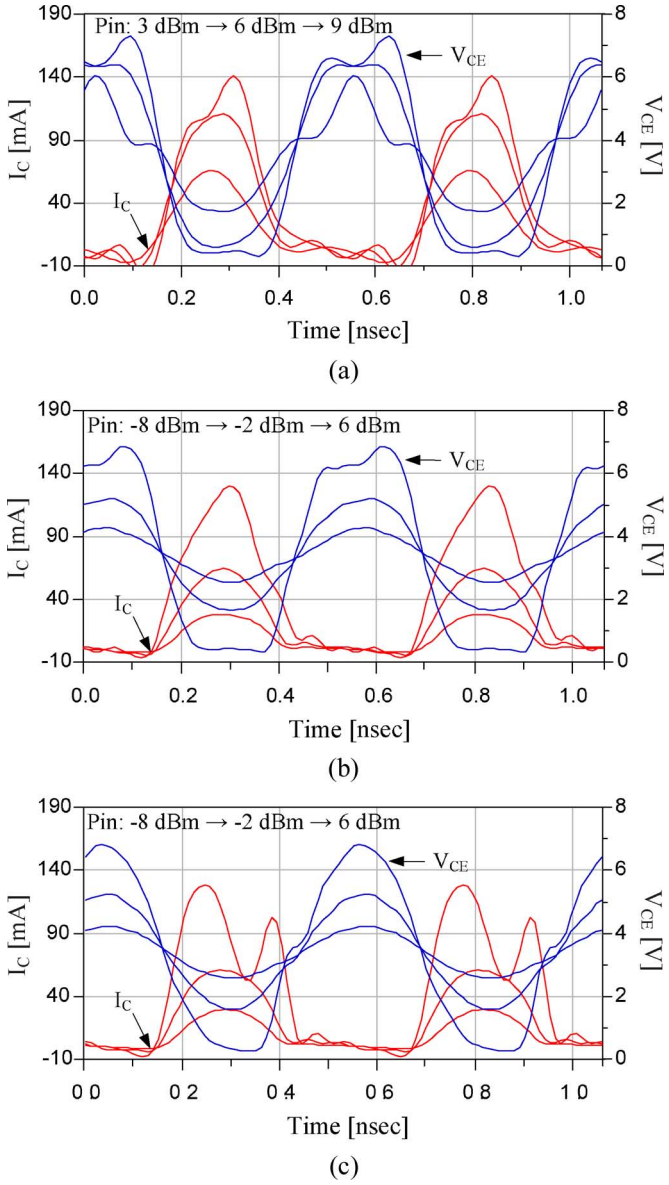

Fig. 8. Voltage and current waveforms of the each power cell. (a) Class-F operation of the class-AB/F PA. (b) Class-AB operation of the class-AB/F PA. (c) Conventional class-AB PA.

stability of the power stage, given by a large-signal S-parameter test [17]. Both operations are stable before an input enters the PA. When an input turns on and saturates the PA in the class-F mode, the PA is unstable. The class-F operation of the PA becomes stable with R_B of 1 Ω. The design goal of the PA is a multimode operation for an IS-95A CDMA and a PCS1900 GSM signals in the PCS band, i.e., 1.85–1.91 GHz. Over 32 dBm of saturated maximum power is required for PCS1900 PAs and over 31 dBm of the $P1$ dB output power for the CDMA system. Thus, the PA is designed to drive over 31.2 dBm of $P1$ dB output power. The supply voltage is 3.4 V and the knee voltage of the device is approximately 0.4 V. For the class-AB operation, the fundamental load is determined by (9). The conduction angle $\alpha_{\rm AB}$ is determined such that the PA under the class-AB operation is as efficient as possible while satisfying the linearity requirement. $\alpha_{\rm AB}$ is at a class-AB bias level. For the class-F operation, $\alpha_{\rm F}$ is close to π. For the fundamental load, tradeoffs in performance should be considered for the class-AB and class-F operations. Fig. 6 shows how to determine the fundamental load $R_{1\_{\rm AB/F}}$ for the multimode operation. The fundamental load is selected to maximize the performances of PAE and output power under class-F operation while satisfying the linearity of class-AB operation. The IMD3 needs to be below −30 dBc at 28 dBm of output power for the class-AB operation. Thus, 4.2 Ω of the fundamental load is selected for the multimode operation. Table I shows the values of the matching circuit elements for the class-AB/F PA.

B. Simulated Performance Comparison

Two modes of the class-AB/F PA and conventional class-AB PA are simulated for comparison. The conventional class-AB PA has the second harmonic control circuit without the third harmonic control circuit. Their fundamental load impedances are identical to 4.2 Ω. The operations of the class-AB/F PA are achieved by changing only $V_{\rm MODE}$ of the bias circuit—the idle

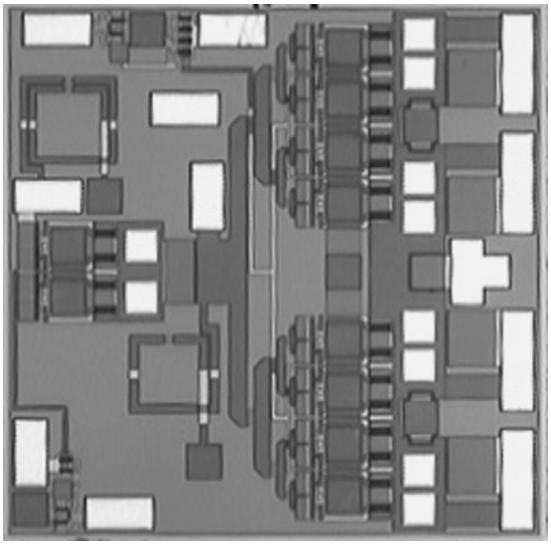

Fig. 9. Chip photograph.

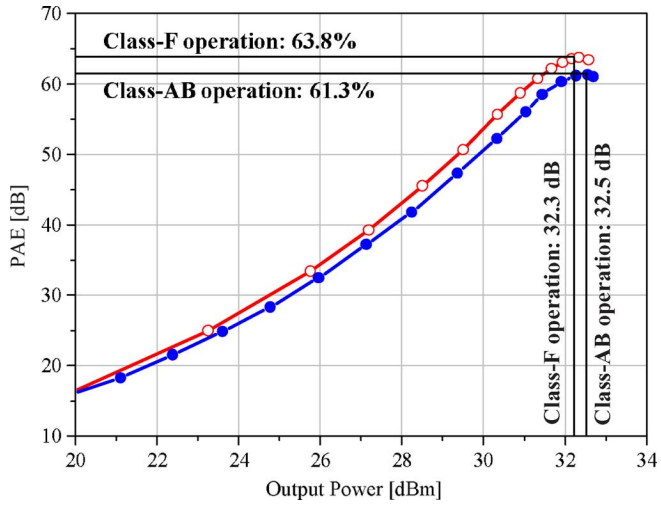

Fig. 10. Measured CW tests for the class-F and class-AB operations. Supply voltages of 3.4 V, and idle currents of 72 and 0.8 mA for the class-AB and class-F operations.

currents for the class-AB and class-F operations are 55 and 0.8 mA, respectively.

Fig. 7(a) shows the performance of the PAs. The class-AB operation of the PA with the third harmonic control circuit has a maximum PAE approximately 9.2% higher than the conventional class-AB PA. The maximum PAE of the class-F operation is 65%, which is 3% higher than that of the class-AB operation of the PA. The gain of the class-F operation is lower than that of the class-AB operation because of the lower bias. Due to the third harmonic control circuit, the class-AB operation produces an output power 0.4 dB greater than the conventional class-AB PA. The class-AB operation generates an output power 0.3 dB higher than the class-F operation of the PA. Fig. 7(b) shows the linearity of the PAs. The IMD3 of the class-AB operation follows that of the conventional class-AB PA, while IMD5 is increased by one or two decibels owing to the third harmonic control circuit described earlier in Section II-B. The voltage and current waveforms illustrated in Fig. 8 are helpful in understanding the operation of the class-AB/F PA and the effect of the third harmonic control circuit. The nonlinearity of class-F operation caused by the bias close to a class B is shown in Fig. 8(a). The PA operates nonlinearly and has the wrong phase relationship of voltage harmonics at a low power ($P\mathrm{in} = 3\,\mathrm{dBm}$). However, when the device generates more harmonics due to the nonlinear behavior, the third harmonic control circuit causes a flat voltage waveform, which has close to 180° of phase difference between the fundamental and third harmonic voltage components. The second harmonic of the voltage waveform is suppressed by the *L–C* series resonant circuit, while the third harmonic of the voltage waveform is enhanced by the *L–C* parallel resonant circuit. Fig. 8(b) shows the waveforms for the class-AB operation of the class-AB/F PA. The waveforms at a low power are sinusoidal, which enables the linear operation. The voltage waveform in the high power region is square so that it enhances the efficiency. Fig. 8(c) shows the conventional class-AB PA without the third harmonic circuit. It operates linearly in a low power region. The current waveform in the saturated power region is affected by the third harmonic induced, which is not suppressed. The voltage waveform maintains a round shape such that the efficiency of the PA is lower than the others.

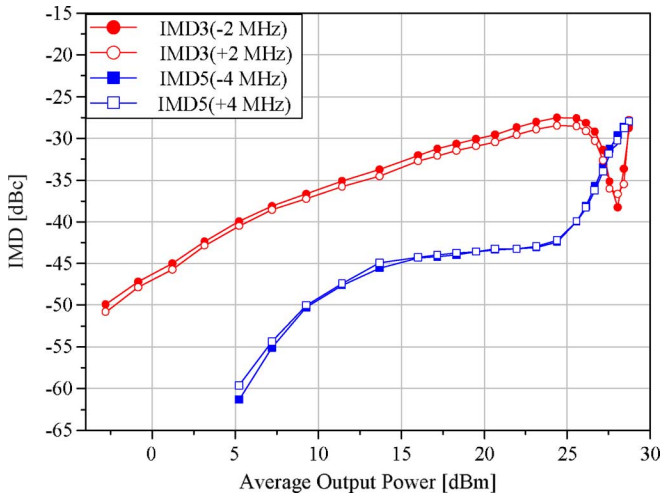

Fig. 11. Measured IMD characteristics of the class-AB/F PA under the class-AB operation.

IV. Implementation and Experimental Results

The class-AB/F PA is fabricated by an InGaP/GaAs 2-μm HBT process. The PA is integrated in a chip with the die size of $1.2 \times 1.2\ \mathrm{mm}^2$, except for two capacitors of the output matching circuit, a photograph of which is presented in Fig. 9. The inductance for the third harmonic circuit is implemented by a slab inductor instead of a spiral inductor. The slab inductor has a higher Q-factor than the spiral inductor [19], achieving higher third harmonic impedance and lower loss. A capacitor is implemented on the chip for the second harmonic control circuit, and the gold bond wires complete the *L–C* series circuit.

The chip is assembled on a two-layer FR-4 board and a continuous wave (CW) signal is applied to the class-AB/F PA using Agilent's E4433B signal generator. The performances of the class-AB and class-F operations are measured and depicted in Fig. 10. The operating frequency is set at 1.88 GHz, which is the center of the PCS band of 1.85–1.91 GHz. For the class-AB bias, the dc supply voltage is 3.4 V, and the idle current is 72 mA with V_{MODE} of 2.9 V. The class-AB operation has PAE of

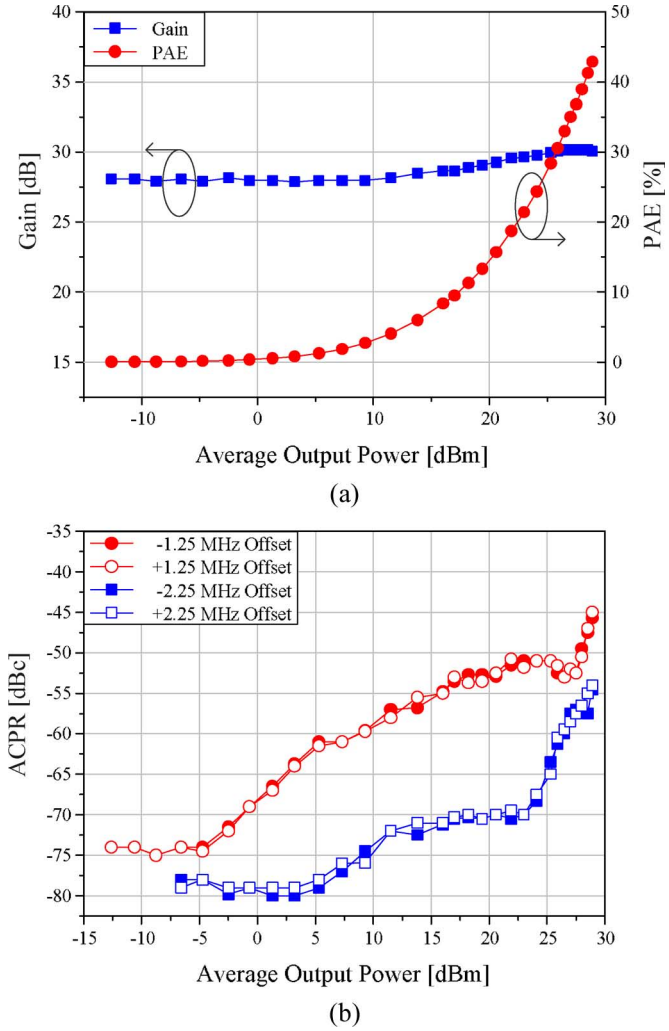

Fig. 12. Measured performance of the class-AB operation for an IS-95A CDMA signal. (a) Gain and PAE. (b) ACPR.

59.5% and 61.3% at 31.5 dB of $P1$ dB and 32.5 dB of P_{SAT}, respectively. The maximum power and the PAE of the class-F operation are 32.3 dBm and 63.8%, respectively. These results show that the class-F operation delivers less power and higher PAE than the class-AB operation. The intermodulation distortion (IMD) characteristics of the class-AB operation are measured using a two-tone signal with 2-MHz tone spacing, and they are depicted in Fig. 11. The class-AB/F topology with the third harmonic control circuit does not deteriorate the IMD3 characteristics, and the IMD5 characteristic is degraded a little due to the third control circuit, but its effect is not serious. The result of IMDs clearly shows that the class-AB operation is an adequate linear amplifier. A modulated signal reverse-link IS-95A CDMA with a chip rate of 1.2288 Mc/s at 1.88 GHz is tested to verify the class-AB operation in the real environment, and the test result is illustrated in Fig. 12. The gain and PAE are 30.5 dB and 38.9%, respectively, at the average output power of 28 dBm. The ACPRs are below −49.5 and −56.5 dBc at the offsets of 1.25 and 2.25 MHz, respectively, for the average output power of 28 dBm and below. For the class-F operation measured for a PCS1900 GSM input signal, the highest PAE is 64.7% at the 32.5-dBm output power with a 3.5-V dc supply

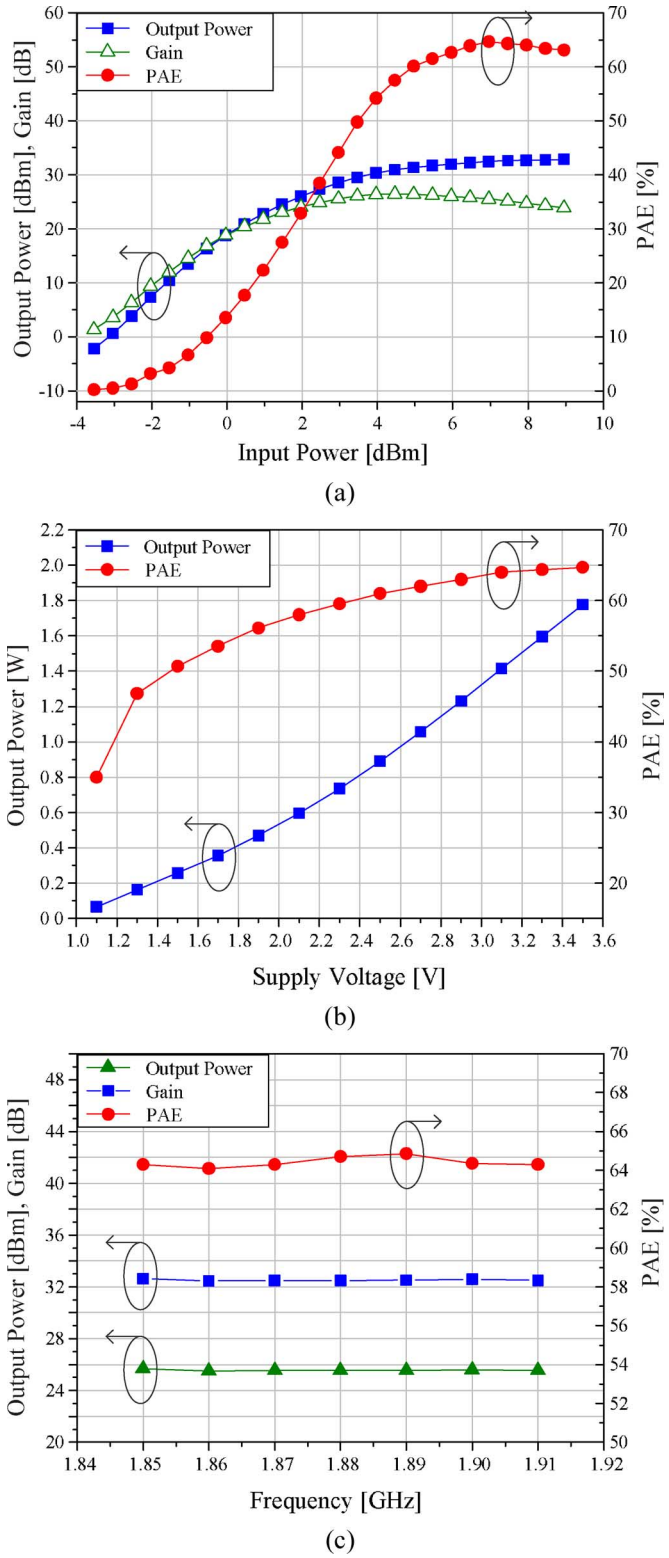

Fig. 13. Measured performances of the class-F operation for a PCS1900 GSM signal. (a) Gain and PAE. (b) Sweep of supply voltage with a constant input power. (c) Sweep of frequency across the bandwidth of the signal.

voltage, as shown in Fig. 13(a). The idle current is 0.8 mA with V_{MODE} of 2.45 V. In Fig. 13(b), the output power and PAE at the input power of 7 dBm are shown as a function of the dc supply voltage [18], and Fig. 13(c) shows the responses of the PA across the PCS frequency band. Table II shows the measured

TABLE II
MEASURED HARMONICS POWER OF CLASS-AB/F PA

Signal(mode)	Pout [dBm]	$2f_0$ [dBc]	$3f_0$ [dBc]
IS-95A (class-AB mode)	28	–48	–47
PCS1900 (class-F mode)	32.5	–44.3	–35

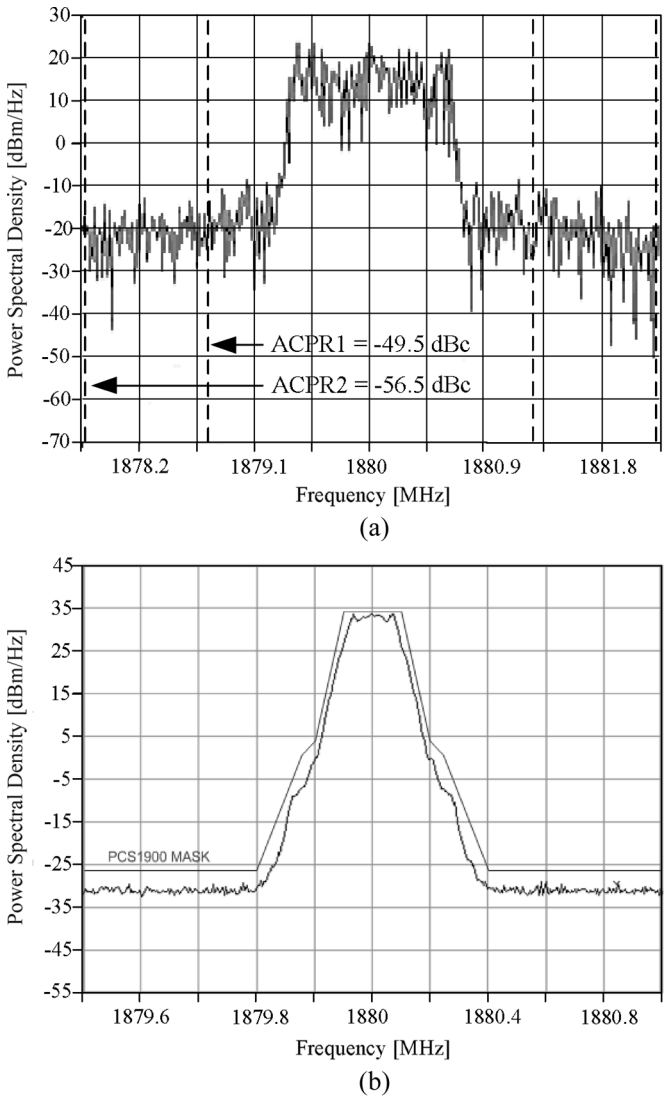

Fig. 14. Measured output spectra. (a) For a reverse-link IS-95A CDMA signal. Channel bandwidth is 1.25 MHz and resolution bandwidth is 30 kHz. (b) For a PCS1900 GSM signal.

harmonics power at the each mode of PA. Due to the harmonics control circuit, low harmonics power is measured in both modes of the PA. The class-F operation delivers more harmonics than the class-AB operation because of lower bias. Fig. 14(a) and (b) shows the output spectra of the class-AB/F PA for each signal. The class-AB operation performs appropriately for an IS-95A CDMA signal at the average output power of 28 dBm satisfying the linearity specification of -44 and -52 dBc at the offsets of 1.25 and 2.25 MHz, respectively. The spectrum of output power for a PCS1900 GSM signal is also sufficiently covered by the spectrum mask over the full range of output power. In Table III, the performance of class-AB operation is compared with that of other PAs for a CDMA signal in the PCS band, and in Table IV, the class-F operation of the class-AB/F PA is compared with other comparable PAs. These results allow us to conclude that the class-AB/F PA has an acceptable performance for the multimode applications.

TABLE III
PERFORMANCE COMPARISON WITH CLASS-AB OPERATION OF CLASS-AB/F PA

PA	Vs [V]	Pout [dBm]	PAE [%]	ACPR1 [dBc]	ACPR2 [dBc]
[20]	3.4	28	38.13	–50	·
[16]	3.4	30	39.5	–46	·
[21]	3.4	28	35.2	–45	·
This work	3.4	28	38.9	–49.5	–56.5

[1] for a reverse-link CDMA signal in the PCS band

[2] fabricated using InGap/GaAs HBT process

TABLE IV
PERFORMANCE COMPARISON WITH CLASS-F OPERATION OF CLASS-AB/F PA

PA	Signal	Vs [V]	Pout [dBm]	PAE [%]	Process (HBT)
[22]	1.8-GHz	3	33	62	AlGaAs
[23]	1.95-GHz	3.3	27	62.5	GaAs
[24]	GSM900	3.6	34.8	63	HBT
This work	PCS1900	3.5	32.5	64.7	InGaP/GaAs

V. CONCLUSIONS

We have proposed a new concept of a class-AB/F PA for multimode operation. The class-F operation of the PA is highly efficient and comparable to the class-F PA. The class-AB operation is also highly efficient and linear because it is a standard class-AB PA, but with the third harmonic open circuit. The open circuit generates a little fifth harmonic, but the efficiency and power density are enhanced. The proper multimode operation is achieved by selecting an intermediate fundamental load that considers the two modes of operation. The simulation results show that the class-AB operation of the class-AB/F PA has a PAE 9.2% higher than the conventional class-AB PA, which does not deteriorate the IMD characteristics. The PAE of the class-F operation is found to be 3% higher than that of class-AB operation of the PA. The PA is implemented by an InGaP/GaAs HBT process to demonstrate the operations and tested. The class-F operation has a maximum PAE of 64.7% measured at 32.5-dBm output power for a PCS1800 GSM signal, while the class-AB operation has a PAE of 38.9% and the adjacent channel power ratios (ACPRs) of -49.5 and -56.5 dBc at the offsets of 1.25 and 2.25 MHz, respectively, are measured at the average output power of 28 dBm for an IS-95A CDMA signal. These results show clearly that the class-AB/F PA is a good candidate for the multimode PA of the next-generation wireless communication systems.

ACKNOWLEDGMENT

The authors would like to thank Wireless Power Amplifier Module (WiPAM) Inc., Seongnam, Gyeongi, Korea, for the advice and the chip fabrication. The authors would also like to acknowledge the support of Dr. H. Park, K. Lee, and H. Jung, all with the Pohang University of Science and Technology (POSTECH), Pohang, Gyungbuk, Korea.

REFERENCES

[1] L. Zhen, Z. Wenan, S. Junde, and H. Chunping, "Consideration and research issues for the future generation of mobile communication," in *Proc. IEEE Can. Elect. Comput. Eng. Conf.*, Mar. 2002, vol. 6, no. 1, pp. 44–55.

[2] B. Bing and N. Jayant, "A cellphone for all standards," *IEEE Spectr.*, vol. 39, no. 5, pp. 34–39, May 2002.

[3] B. Bakkaloglu and P. A. Fontaine, "Multi-mode, multi-band RF transceiver circuits for mobile terminals in deep-submicron CMOS processes," in *Proc. IEEE Radio Freq. lntegrated Circuits Symp.*, Jun. 2005, pp. 483–486.

[4] E. McCune, "High-efficiency, multi-mode, multi-band terminal power amplifiers," *IEEE Micro*, vol. 6, no. 1, pp. 44–55, Mar. 2005.

[5] P. D. Tseng, L. Zhang, G. B. Gao, and M. F. Chang, "A 3-V monolithic SiGe HBT power amplifier for dual-mode (CDMA/AMPS) cellular handset applications," *IEEE J. Solid-State Circuits*, vol. 35, no. 9, pp. 1338–1344, Sep. 2000.

[6] S. Maeng, S. Chun, J. Lee, C. Lee, K. Youn, and H. Park, "A GaAs power amplifier for 3.3 V CDMA/AMPS dual-mode cellular phones," *IEEE Trans. Microw. Theory Tech.*, vol. 43, no. 12, pp. 2839–2844, Dec. 1995.

[7] S. C. Cripps, *Advanced Techniques in RF Power Amplifier Design*. Norwood, MA: Artech House, 2002.

[8] F. H. Raab, "Class-F power amplifiers with maximally flat waveforms," *IEEE Trans. Microw. Theory Tech.*, vol. 45, no. 11, pp. 2007–2012, Nov. 1997.

[9] C. Duvanaud, S. Dietsche, G. Pataut, and J. Obregon, "High-efficient class F GaAs FET amplifiers operating with very low bias voltages for use in mobile telephones at 1.75 GHz," *IEEE Microw. Guided Wave Lett.*, vol. 3, no. 8, pp. 40–48, Aug. 1993.

[10] P. Colantonio, F. Giannini, G. Leuzzi, and E. Limiti, "On the class-F power amplifier design," *Int. J. RF Microw. Comput.-Aided Eng.*, vol. 9, no. 2, pp. 129–149, 1999.

[11] P. Colantonio, J. A. Garcia, F. Giannini, C. Gomez, N. B. Carvalho, E. Limiti, and J. C. Pedro, "High efficiency and high linearity power amplifier design," *Int. J. RF Microw. Comput.-Aided Eng.*, vol. 15, no. 5, pp. 453–468, 2005.

[12] W. Kim, S. Kang, K. Lee, M. C. Chung, J. Kang, and B. Kim, "Analysis of nonlinear behavior of power HBTs," *IEEE Trans. Microw. Theory Tech.*, vol. 50, no. 7, pp. 1714–1722, Jul. 2002.

[13] W. Kim, S. Kang, K. Lee, M. C. Chung, Y. Yang, and B. Kim, "The effects of Cbc on the linearity of AlGaAs/GaAs power HBTs," *IEEE Trans. Microw. Theory Tech.*, vol. 49, no. 7, pp. 1270–1276, Jul. 2001.

[14] Y. Y. Woo, Y. Yang, and B. Kim, "Analysis and experiments for high efficiency class-F and inverse class-F power amplifiers," *IEEE Trans. Microw. Theory Tech.*, vol. 54, no. 5, pp. 1969–1974, May 2006.

[15] S. Gao, "High-efficiency class-F RF/microwave power amplifiers," *IEEE Micro*, vol. 7, no. 1, pp. 40–48, Feb. 2006.

[16] Y. Noh and C. Park, "PCS/W-CDMA dual-band MMIC power amplifier with a newly proposed linearizing bias circuit," *IEEE J. Solid-State Circuits*, vol. 37, no. 9, pp. 1096–1099, Sep. 2002.

[17] M. L. Edwards and J. H. Sinsky, "New criterion for linear 2-port stability using a single geometrically derived parameter," *IEEE Trans. Microw. Theory Tech.*, vol. 40, no. 12, pp. 2303–2311, Dec. 1992.

[18] K. C. Tsai and P. R. Gray, "A 1.9-GHz 1-W CMOS class-E power amplifier for wireless communications," *IEEE J. Solid-State Circuits*, vol. 34, pp. 962–970, Jul. 1999.

[19] I. Aoki, S. Kee, D. Rutledge, and A. Hajimiri, "Fully integrated CMOS power amplifier design using the distributed active-transformer architecture," *IEEE J. Solid-State Circuits*, vol. 37, no. 3, pp. 371–383, Mar. 2002.

[20] Y. Yang, "High pass output matching technique with enhanced third harmonic rejection for CDMA power amplifiers," in *IEEE MTT-S Int. Microw. Symp. Dig.*, Jun. 2005, pp. 2051–2054.

[21] J. Kim, Y. Noh, and C. Park, "A bias controlled HBT MMIC power amplifier with improved PAE for PCS applications," in *Proc. Int. Microw. Millimeter-Wave Technol. Conf.*, Aug. 2002, pp. 725–728.

[22] J. Muller, P. Baureis, O. Berger, T. Boettner, N. Bovolon, R. Schultheis, G. Packeiser, and P. Zwicknagl, "A small chip size 2 W, 62% efficient HBT MMIC for 3 V PCN applications," *IEEE J. Solid-State Circuits*, vol. 33, no. 9, pp. 1277–1283, Sep. 1998.

[23] E. A. Jarvinen and M. J. Alanen, "GaAs HBT class-E amplifiers for 2-GHz mobile applications," in *Proc. Radio Freq. lntegrated Circuits Symp.*, Jun. 2005, pp. 421–424.

[24] R. Koller, A. Stelzer, K. Abt, A. Springer, and R. Weigel, "A class-E GSM-handset PA with increased efficiency," in *Proc. 2003 33rd Eur. Microw. Conf.*, Oct. 2003, vol. 1, pp. 257–260.

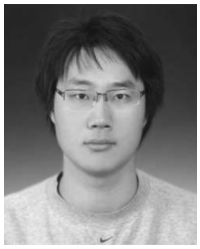

Daehyun Kang received the B.S. degree in electronic and electrical engineering from Kyungpook National University, Daegu, Korea, in 2006, and is currently working toward the Ph.D. degree at the Pohang University of Science and Technology (POSTECH), Pohang, Gyungbuk, Korea.

His main research interests are RF circuits for wireless communications, especially highly efficient and linear RF transmitters and RF PA design.

Daekyu Yu received the B.S. degree in electrical engineering from Hanyang University, Seoul, Korea, in 2001, and the Ph.D. degree from the Pohang University of Science and Technology (POSTECH), Pohang, Gyungbuk, Korea, in 2007.

In 2007, he founded Wireless Power Amplifier Module (WiPAM) Inc., Seongnam, Gyeunggi, Korea. His research interests include the design of highly efficient and linear RF PAs for fourth–generation (4G) wireless communication and high-speed optimization of InP-based HBTs.

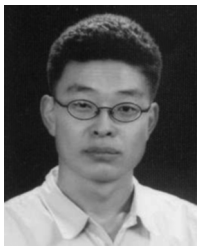

Kyoungjoon Min received the B.S. degree in electronic engineering from the Pohang University of Science and Technology (POSTECH), Pohang, Gyungbuk, Korea, in 2005, and is currently working toward the Ph.D. degree in electrical engineering at POSTECH.

In 2007, he founded the Wireless Power Amplifier Module (WiPAM) Inc., Seongnam, Gyeunggi, Korea. His research interests include highly linear and efficient RF PA for 4G mobile communication.

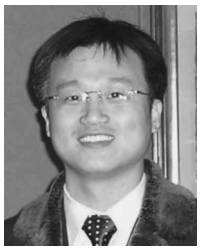

Kichon Han received the B.S. and M.S. degrees in electrical engineering from the Pohang University of Science and Technology (POSTECH), Pohang, Gyungbuk, Korea, in 1996 and 1998, respectively, and is currently working toward the Ph.D. degree at POSTECH.

From 2000 to 2006, he was with Future Communications IC (FCI) Inc., Seongnam, Gyeongi, Korea, where he designed PAs and transceivers for cellular handsets. His interests include GaAs HBT RF PAs and SiGe HBT RF transceivers.

Jinsung Choi (S'07) received the B.S. degree in electrical engineering from the Pohang University of Science and Technology (POSTECH), Pohang, Gyungbuk, Korea, in 2004, and is currently working toward the Ph.D. degree at POSTECH.

His main research interests are CMOS RF circuits for wireless communications, mixed-mode signal-processing integrated-circuit design, and highly efficient and linear RF transmitter architectures.

Dongsu Kim received the B.S. degree in electrical engineering from the Pohang University of Science and Technology (POSTECH), Pohang, Gyungbuk, Korea, in 2007 and is currently working toward the Ph.D. degree at POSTECH.

His research interests are CMOS RF circuits for wireless communications with a focus on highly efficient and linear RF transmitter design.

Boshi Jin received the B.S. and M.S. degrees in electrical and communication engineering from the Harbin Institute of Technology, Harbin, China, in 2003 and 2005, respectively, and is currently working toward the Ph.D. degree at the Pohang University of Science and Technology (POSTECH), Pohang, Gyungbuk, Korea.

His current research interests include the fully integrated RF CMOS PA and its linearity techniques.

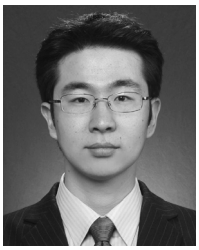

Myoungsu Jun received the B.S. degree in electrical and computer engineering from Pusan National University, Pusan, Korea, in 2007, and is currently working toward the Ph.D. degree at the Pohang University of Science and Technology (POSTECH), Pohang, Gyungbuk, Korea.

His current research interests include highly efficient CMOS RF PA design.

Bumman Kim (M'78–SM'97–F'07) received the Ph.D. degree in electrical engineering from Carnegie–Mellon University, Pittsburgh, PA, in 1979.

From 1978 to 1981, he was engaged in fiber-optic network component research with GTE Laboratories Inc. In 1981, he joined the Central Research Laboratories, Texas Instruments Incorporated, where he was involved in development of GaAs power field-effect transistors (FETs) and monolithic microwave integrated circuits (MMICs). He has developed a large-signal model of a power FET, dual-gate FETs for gain control, high-power distributed amplifiers, and various millimeter-wave MMICs. In 1989, he joined the Pohang University of Science and Technology (POSTECH), Pohang, Gyungbuk, Korea, where he is a Namko Professor with the Department of Electrical Engineering, and Director of the Microwave Application Research Center, where he is involved in device and circuit technology for RF integrated circuits (RFICs). He was a Visiting Professor of electrical engineering with the California Institute of Technology, Pasadena, in 2001. He has authored over 200 technical papers.

Dr. Kim is a member of the Korean Academy of Science and Technology and the Academy of Engineering of Korea. He was an associate editor for the IEEE TRANSACTIONS ON MICROWAVE THEORY AND TECHNIQUES and a Distinguished Lecturer of the IEEE Microwave Theory and Techniques Society (IEEE MTT-S).